

Conductance distribution in 3D Anderson insulators: deviation from log-normal form

P. MARKOŠ¹(*), K. A. MUTTALIB², P. WÖLFLE³ and J. R. KLAUDER²(**)

¹ *Institute of Physics, Slovak Academy of Sciences - 845 11 Bratislava, Slovakia*

² *Department of Physics, University of Florida, Gainesville, FL 32611-8440*

³ *Institut für Theorie der Kondensierten Materie, Universität Karlsruhe, Germany*

PACS. 73.23.-b – Electronic transport in mesoscopic systems.

PACS. 71.30.+h – Metal-insulator transitions and other electronic transitions.

PACS. 72.10.-d – Theory of electronic transport; scattering mechanisms.

Abstract. – We show how a recent proposal to obtain the distribution of conductances in three dimensions (3D) from a generalized Fokker-Planck equation for the joint probability distribution of the transmission eigenvalues can be implemented for all strengths of disorder by numerically evaluating certain correlations of transfer matrices. We then use this method to obtain analytically, for the first time, the 3D conductance distribution in the insulating regime and provide a simple understanding of why it differs qualitatively from the log-normal distribution of a quasi one-dimensional wire.

It has been shown recently that for a quasi one-dimensional (Q1D) disordered quantum wire, the distribution of conductances $P(g)$ (at zero temperature, in the absence of electron-electron interaction) has many surprising features arising from large mesoscopic fluctuations. These include a highly asymmetric ‘one-sided’ log-normal distribution at intermediate disorder between the metallic and insulating limits [1,2], and a singularity in the distribution near the dimensionless conductance $g \sim 1$ in the insulating regime [3]. Although there is no phase transition in Q1D conductors, numerical studies support the conjecture that some of these features persist in higher dimensions as well [4,5], which may have important consequences for the Anderson metal-insulator transition in three dimensions (3D) [6]. However, while a systematic method has recently been developed to obtain analytically the full $P(g)$ in Q1D [7], no such method is yet available in higher dimensions. Indeed, it has not been possible so far to study analytically even the simpler case of the distribution $P(g)$ for a 3D insulator [8,9].

A phenomenological generalization of the Q1D method to study the distribution of conductances in higher dimensions has been proposed recently [10]. For a given dimensionality, the generalization involves an unknown matrix K to be determined from numerical studies of the properties of transmission matrices for conductors of various strengths of disorder. Within a set of well-defined approximations, this method is applicable in principle for all strengths of disorder in all dimensions. In the present work we first of all test these approximations and

(*) E-mail: markos@savba.sk

(**) Also at Department of Mathematics.

show that they are valid in 3D. We then study the matrix K in 3D and show that it can be modeled reasonably well by a single parameter in both the metallic and insulating limits, and that it contains information about the critical regime. We find that while the value of the parameter in the metallic regime in 3D remains the same as in Q1D, it changes dramatically across the transition and in the insulating regime. This implies that while the 3D metal is similar to a Q1D metal, the localization in 3D is qualitatively different from the localization in Q1D, discussed in Refs. [1-3]. We use the value of the parameter in the insulating limit to obtain analytically, for the first time, the full $P(g)$ of a 3D insulator. We show e.g. that the density of Lyapunov exponents in 3D is qualitatively different from that in Q1D; while the conductance in the insulating regime is dominated by the smallest Lyapunov exponent in Q1D, this is no longer true for 3D. The resulting 3D $P(g)$ is *not* log-normal even in the deeply insulating regime. Our results are in agreement with direct numerical studies.

The distribution of conductances in Q1D was obtained within the transfer matrix approach. In this approach, a conductor of length L_z and width $L \times L$ is placed between two perfect leads; the scattering states at the Fermi energy then define $N \propto L^2$ channels. The $2N \times 2N$ transfer matrix M relates the flux amplitudes on the right of the system to those on the left [11]. Flux conservation and time reversal symmetry (we consider the case of unbroken time reversal symmetry only) restricts the number of independent parameters of M to $N(2N + 1)$ and M can be written in general as [12]

$$M = \begin{pmatrix} u & 0 \\ 0 & u^* \end{pmatrix} \begin{pmatrix} \sqrt{1+\lambda} & \sqrt{\lambda} \\ \sqrt{\lambda} & \sqrt{1+\lambda} \end{pmatrix} \begin{pmatrix} v & 0 \\ 0 & v^* \end{pmatrix}, \quad (1)$$

where u, v are $N \times N$ unitary matrices, and λ is a diagonal matrix, with positive elements $\lambda_i, i = 1, 2, \dots, N$. The restriction of the approach to Q1D arises from the ‘‘isotropy’’ approximation, that the distribution $p_{L_z}(M)$ is independent of the matrices u and v . In [10], this restriction was lifted in favor of an unknown phenomenological matrix

$$K_{ab} \equiv \langle k_{ab} \rangle_L; \quad k_{ab} \equiv \sum_{\alpha}^N |v_{a\alpha}|^2 |v_{b\alpha}|^2, \quad (2)$$

where the angular bracket represents an ensemble average [13]. In terms of this matrix, the distribution $p_{L_z}(M)$ satisfies an evolution equation given by [10]

$$\frac{\partial p_{L_z}(\lambda)}{\partial(L_z/l)} = \frac{1}{\bar{J}} \sum_a^N \frac{\partial}{\partial \lambda_a} \left[\lambda_a (1 + \lambda_a) K_{aa} \bar{J} \frac{\partial p}{\partial \lambda_a} \right], \quad \bar{J} \equiv \prod_{a < b}^N |\lambda_a - \lambda_b|^{\gamma_{ab}}; \quad \gamma_{ab} \equiv \frac{2K_{ab}}{K_{aa}}. \quad (3)$$

In Q1D, the matrix K reduces to $K_{ab} = \frac{1+\delta_{ab}}{N+1}$, which implies $\gamma_{ab} = 1$, and one recovers the well known DMPK equation with the symmetry parameter $\beta = 1$ [12]. In 3D, K is not known analytically. We obtain it from direct numerical studies of a tight binding Anderson model defined by the Hamiltonian

$$\mathcal{H} = W \sum_n \varepsilon_n c_n^\dagger c_n + \sum_{[nn']} t_{nn'} c_n^\dagger c_{n'}. \quad (4)$$

In (4), $n = (xyz)$ counts sites on the lattice of the size $L \times L \times L_z$, and ε_n are random energies, uniformly distributed in the interval $[-\frac{1}{2}, \frac{1}{2}]$. The parameter W measures the strength of the disorder. The Fermi energy is chosen as $E_F = 0.01$. The hopping term $t_{nn'}$ between the nearest-neighbor sites nn' is unity for hopping along the z direction and $t_{nn'} = t$ for hopping

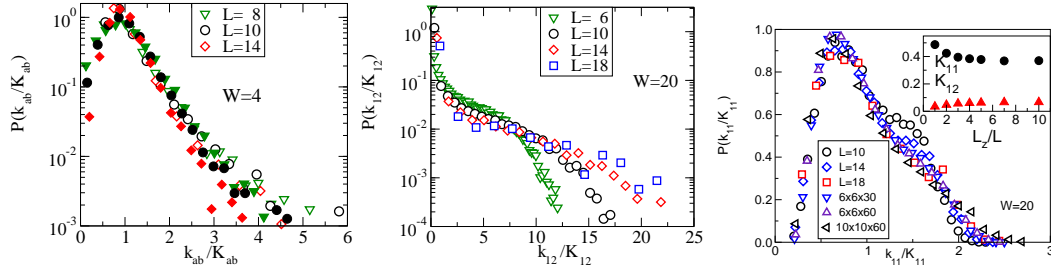


Fig. 1 – Left: the distributions of *normalized* parameters k_{11} (open symbols) and k_{12} (full symbols) in the metallic regime ($W = 4$). Two right figures show the same for the insulator ($W = 20$). Inset of right figure shows K_{11} and K_{12} of systems $6 \times 6 \times L_z$ as a function of L_z .

in the x and y directions. To avoid closed channels existing in perfect leads, we use $t = 0.4$. Then the model (4) exhibits a metal-insulator transition at $W_c \approx 9$. In order to construct a simple model for the matrix K , we use the method of [14] to calculate numerically the matrix TT^\dagger (T is the transmission matrix). Using Eq. (1), we have $TT^\dagger = v^*(1 + \lambda)^{-1}v$. Diagonalization of TT^\dagger gives us both λ and all elements of the matrix v .

There are two major assumptions made in [10] in deriving Eq. (3), (i) the elements k_{ab} can be replaced by their mean values K_{ab} and (ii) the L_z -dependence of K_{ab} is negligible. To test these assumptions, we analyzed the probability distributions $P(k_{ab}/K_{ab})$ in the insulating regime and compared them with those for metals (figure 1). In the metallic regime all distributions seem to be self-averaging (they become narrower when L increases), with sharp maximum at 1. In the insulating regime $P(k_{12}/K_{12})$ has a very sharp distribution too, but possesses a long exponential tail to values $k_{12} \gg K_{12}$. $P(k_{11}/K_{11})$ is broader, with variance of the same order as the mean. This means that while assumption (i) remains valid to leading order, fluctuations in the diagonal elements k_{aa} in the insulating regime can be important if the final results are sensitive to the exact values of the parameters. We will therefore concentrate on the qualitative features of the distribution of conductances, which are insensitive to those fluctuations. Figure 1 also shows that K_{ab} depend slightly on the ratio L_z/L and reach L_z -independent limiting values when $L_z/L \rightarrow \infty$. This is qualitatively consistent with assumption (ii) and agrees with previous numerical analysis of parameters x_i ($\lambda_i \equiv \sinh^2 x_i$) [15,16]. We therefore conclude that at least to leading approximation, the generalized DMPK equation (3) can be used in 3D at all disorder strengths.

We now construct a model for the matrix K in the insulating regime. Figure 2 shows K_{aa} as a function of a and γ_{ab} for different (a, b) in this regime. While there is some dependence on the indices for both K and γ , the dependence is weak compared to the dependence of the matrix elements on disorder in the $L \rightarrow \infty$ limit. As only few channels contribute to the conductance in the insulating regime, we will ignore this index dependence and use $K_{aa} \approx K_{11}$ and $\gamma_{ab} \approx \gamma_{12}$ [17]. Figure 3 is consistent with $K_{11} \propto 1/L^m$, where $m = 2, 1, 0$ in the metallic, critical and insulating limits, respectively, in agreement with [18]. Figure 3 also shows γ_{12} as a function of disorder. It is unity in the weakly disordered metallic regime, showing the same behavior as in the Q1D limit. This is true for all γ_{ab} , which implies that a 3D metal is very similar to a Q1D metal. However, as the disorder is increased for given L , the value of γ_{12} starts to decrease. Several plots with different L values show that in the insulating limit $\gamma_{12} \propto 1/L$ (right figure 3). Thus our data show that the behavior of *strongly disordered* insulators differs from that of Q1D systems [8].

While modeling the full γ_{ab} at the critical point needs more careful numerical studies, the

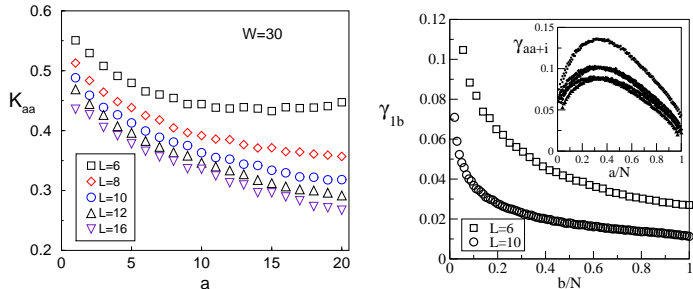


Fig. 2 – Left: a -dependence of K_{aa} for $W = 30$. Right: γ_{ib} for two values of L and (in inset) γ_{aa+i} for $i = 1, 2$ and 3 ($W = 30, L = 10$).

insulating limit is simpler and provides a test case for the generalized DMPK equation (3). It predicts that the logarithmic interaction between the transmission eigenvalues λ_a vanishes as $1/L$ in the insulating limit. In this paper we will test this prediction by evaluating the full distribution of conductances in the insulating limit for a 3D conductor as described by Eq. (3), using the simple approximate model for K suggested by our numerical studies [19], namely

$$K_{aa} \approx K_{11} \approx 1/2\xi \quad \text{and} \quad \gamma_{ab} \approx \gamma_{12} \approx \xi/2L. \quad (5)$$

We can now follow [20] and map the problem onto a Schrödinger equation in imaginary time. The corresponding Hamiltonian contains an interaction term with strength proportional to $\gamma_{12}(\gamma_{12} - 2)$ which vanishes not only for the Q1D unitary case $\gamma_{12} = \beta = 2$ but also in the limit $\gamma_{12} \rightarrow 0$. In the present case, γ_{12} is of order $\xi/2L \ll 1$, and we can neglect the interaction and use the $\beta = 2$ solution of [20]. For $\lambda_a \equiv \sinh^2 x_a$ the distribution is then given by [1]

$$P(g) = \int \prod_a^N dx_a e^{-H} \delta(g - \sum_a h(x_a)); \quad h(x) \equiv \text{sech}^2 x. \quad (6)$$

Here the δ -function represents the Landauer formula for the conductance of a multichannel system [21], and the ‘Hamiltonian’ H is given, in the insulating limit $x_a \gg 1$, by [20]

$$H = - \sum_{a>b}^N \left[\frac{1}{2} \ln |\sinh^2 x_a - \sinh^2 x_b|^{\gamma_{12}} + \ln |x_a^2 - x_b^2| \right] - \sum_{a=1}^N \left[\frac{1}{2} \ln \sinh 2x_a + \ln x_a - \Gamma x_a^2 \right], \quad (7)$$

where $\Gamma \equiv 1/L_z K_{11} \approx 2\xi/L_z \ll 1$. The ratio $\Gamma/\gamma_{12} \approx 4L/L_z$ depends on the geometry, but is independent of disorder, leaving a single independent parameter Γ that determines the strength of disorder. We will use $\Gamma/\gamma_{12} = 4$ appropriate for a cubic system. Note that fluctuations in k_{aa} , ignored in the model, would make the numerical factors in Γ and γ_{12} inaccurate, but will not change either the length or the disorder dependence of these parameters.

The replacement of $\beta = 2$ in [20] by $\gamma_{12} \rightarrow 0$ in Eq. (7) has the consequence that while all $\langle x_a \rangle \gg 1$ in the insulating regime, the difference $s = \langle x_{a+1} - x_a \rangle$ is *not* of the same order as $\langle x_a \rangle$. For example, if we keep only the first two levels, the saddle-point solutions for x_1 and x_2 give $\langle x_1 \rangle \sim L_z/\xi$ and $\langle x_2 - x_1 \rangle \ll \langle x_1 \rangle$. We therefore do not assume that $x_2 \gg x_1$. However, we do make the simplifying approximation that $\ln |\sinh^2 x_a - \sinh^2 x_b| \approx \ln \sinh^2 x_a$

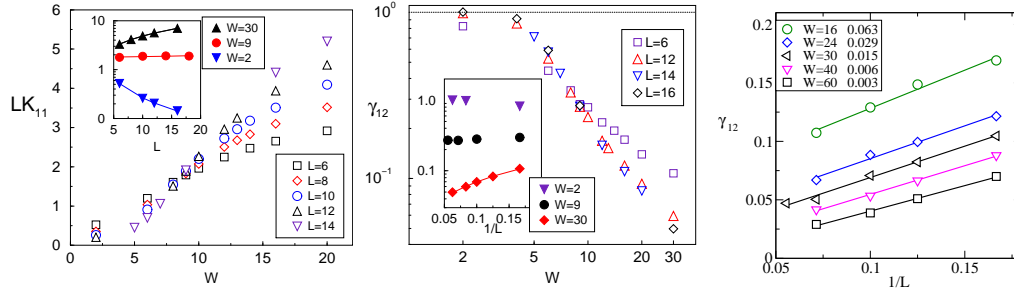


Fig. 3 – Left: LK_{11} for various L as a function of disorder. Note the common crossing point for $W \approx 9$, showing $K_{11} \propto 1/L$ at the critical point. Inset shows the L -dependence of LK_{11} for three values of disorder W . Solid lines are power fits $LK_{11} \propto L^m$ with $m = -1.3, 0.06$ and 0.8 for for $W = 2$ (metal), $W = 9$ (critical point) and $W = 30$ (insulator), respectively. The linear fit for $W = 30$ uses $K_{11} = 0.37 + 1.2/L$. Middle: γ_{12} as a function of disorder for various system sizes. In the metallic regime, $\gamma_{12} \approx 1$. At the critical point, $\gamma_{12} \approx 0.25$. In the localized regime, γ_{12} decreases with increasing W . Inset shows $\gamma_{12}(L)$ for $W = 2, 9$ and 30 . Solid line is a fit $\gamma_{12} = 0.015 + 0.56/L$. Right figure confirms that $\gamma_{12} \propto 1/L$ in the localized regime. Limiting values of $\gamma_{12}(L \rightarrow \infty)$ are given in the legend.

and $\ln|x_a^2 - x_b^2| \approx \ln x_a^2$ for $a > 2$. Eq. (7) then becomes

$$H \approx H_1 + \sum_{a=2}^N [V(x_a) - \gamma_{12}(a-2)f(x_a)], \quad (8)$$

where

$$\begin{aligned} H_1 &= -\ln|x_2^2 - x_1^2| + \Gamma x_1^2 - \frac{1}{2} \ln \sinh 2x_1 - \ln x_1, \\ V(x) &= \Gamma x^2 - \frac{1}{2} \ln \sinh 2x - \ln x - \gamma_{12} \ln \sinh x; \quad f(x) = \ln \sinh x + \frac{2}{\gamma_{12}} \ln x \end{aligned} \quad (9)$$

Following ref [1], we separate out the lowest level x_1 and treat the rest as a continuum with density $\sigma(x)$ beginning at a point $\tilde{x}_2 > x_1$. The corresponding saddle point free energy $F_{sp}(x_1, \tilde{x}_2; g)$ has the form

$$F_{sp}(x_1, \tilde{x}_2) = H_1 - \frac{1}{2\gamma_{12}} \int_{\tilde{x}_2}^b \frac{dx}{f'(x)} [V'^2(x) - \mu_1^2 h'^2(x)], \quad (10)$$

where $\mu_1 = -V'(\tilde{x}_2)/h'(\tilde{x}_2)$ and primes denote x -derivatives. Eq (6) can then be rewritten as

$$P(\ln g) \propto g \int_{\tilde{x}_{2\min}}^b d\tilde{x}_2 e^{-F_{sp}(x_1, \tilde{x}_2; g)} e^{-2(\tilde{x}_2 - x_1)}, \quad (11)$$

where the integration over x_1 is eliminated by a constraint arising from the minimization of the free energy:

$$x_1 = \cosh^{-1}[1/\sqrt{g - g_0}]; \quad g_0 = -\frac{1}{\gamma_{12}} \int_{\tilde{x}_2}^b \frac{dx}{f'(x)} h'(x) [V'(x) + \mu_1 h'(x)]. \quad (12)$$

The lower limit $\tilde{x}_{2\min}$ is the larger of the additional constraints imposed by the conditions $\sigma(\tilde{x}_2) \geq 0$ and $\tilde{x}_2 > x_1 \geq 0$, x_1 real.

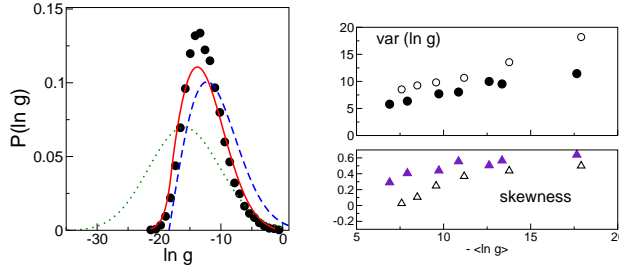


Fig. 4 – Left: Conductance distribution for 3D insulators obtained from direct numerical simulation for $W = 20$, $L = 18$ (circles), and from Eq. (11) for $\Gamma = 0.054$ (solid line). Both have the same mean value $\langle \ln g \rangle = -12.6$. Dashed and dotted lines show Eq. (13) with $\tilde{x}_{2\min} = 1/2\Gamma + 5/8$ and $\tilde{x}_{2\min} = 1/\Gamma$, respectively, with $\Gamma = 0.054$. Right: Comparison of $\text{var}(\ln g)$ and skewness as a function of $\langle \ln g \rangle$ obtained from numerical simulations for various W and L (full symbols) and from present model Eq. (11) (open symbols).

Let us consider first a simple approximate solution of Eq. (11), which is dominated by the lower limit of the integral. To a good approximation, g_0 is negligible compared to g in the insulating limit, and $x_1 \approx \frac{1}{2} \ln(4/g)$. The condition $\sigma(\tilde{x}_2) \geq 0$ gives $\tilde{x}_{2\min} \approx (1 + \Gamma + \gamma_{12})/2\Gamma$ and hence $F_{sp} \approx H_1$. This immediately leads to

$$P(\ln g) \propto (4\tilde{x}_{2\min}^2 - u^2)e^{-\frac{\Gamma}{4}(\frac{1}{\Gamma}+u)^2}, \quad u \equiv \ln(g/4) \quad (13)$$

valid for $|u| < 2\tilde{x}_{2\min}$. Figure 4 shows Eq. (13) compared with the results from direct integration of Eq. (11), both compared with numerical results based on Eq. (4). For the analytic curves, we chose $\Gamma = 0.054$ to have the same $\langle \ln g \rangle$ from Eq. (11) as in the numerical case. Note that using the Q1D result $\gamma_{12} = 1$ gives $\tilde{x}_{2\min} \approx 1/\Gamma$, leading to a log-normal distribution (see dotted line in Figure 4). A saddle point analysis of Eq. (13) allows us to obtain $\langle \ln g \rangle \approx 1/\Gamma - \sqrt{2/\Gamma}$ and $\text{var}(\ln g) \approx 1/\Gamma$, to be compared with the corresponding Q1D results $\langle \ln g \rangle \approx 1/\Gamma$ and $\text{var}(\ln g) \approx 2/\Gamma$. Moreover the skewness $\langle (\ln g - \langle \ln g \rangle)^3 \rangle / [\langle (\ln g - \langle \ln g \rangle)^2 \rangle]^{3/2}$ saturates to a finite value of order unity independent of Γ for $\Gamma \rightarrow 0$, showing the absence of log-normal distribution for 3D insulators even at very strong disorder. Right figure 4 shows variance and skewness calculated from direct integration of Eq. (11) compared to numerical results, consistent with saddle point results from Eq. (13). Quantitative differences between Eq. (11) and numerical results are due to our simplified model Eq. (5), which still overestimates the strength of the interaction for higher channels.

It is instructive to analyze the eigenvalue spectrum in terms of the density $\sigma(x)$. In the insulating phase we find $\sigma(x) \approx 2\Gamma/\gamma_{12} = 8L/L_z$ for $x \gg 2/\gamma_{12}$. This corresponds to a uniform average spacing $s = \langle x_{a+1} - x_a \rangle$ of eigenvalues of order unity ($L = L_z$), compared to the uniform spacing $s \approx L_z/\xi$ in Q1D. In contrast, 3D metals are similar to Q1D metals having uniform $\sigma(x)$ extending down to $x = 0$ and $s \sim L_z/L^2$. The opening of a gap in the spectrum of Lyapunov exponents $\nu_n \equiv \langle x_n \rangle / L_z \sim 1/\xi$ may be considered as the signature of the Anderson transition.

We conclude that Eq. (3) indeed describes a 3D insulator. The solution of Eq. (3), given in Eq. (11) proves the non-trivial asymmetry in the distribution $P(\ln g)$, which is qualitatively distinct from a Q1D insulator. Although such a distribution has been known numerically, our method gives for the first time a simple theoretical understanding of the entire distribution. This opens up the possibility to study analytically in more detail the insulating regime as well as the Anderson transition in 3D in terms of the distribution of conductances, providing

an opportunity to investigate at least qualitatively the nature of a quantum phase transition in the presence of large mesoscopic fluctuations. Numerical work is underway to construct a model for the matrix K at the critical point.

* * *

We acknowledge useful discussions with A.D. Mirlin. KAM is grateful for support from and hospitality at U. Karlsruhe. PW acknowledges support through a Max-Planck Research Award and the Center for Functional Nanostructures of the DFG. PM thanks APVT.

REFERENCES

- [1] MUTTALIB K. A. and WÖLFLE P., *Phys. Rev. Lett.*, **83** (1999) 3013; WÖLFLE P. and MUTTALIB K. A., *Ann. Phys. (Leipzig)*, **8** (1999) 753
- [2] GOPAR V. A. *et al.*, *Phys. Rev. B*, **66** (2002) 174204; FROUFE-PEREZ L. *et al.*, *Phys. Rev. Lett.*, **89** (2002) 246403
- [3] MUTTALIB K. A. *et al.*, *Europhys. Lett.*, **61** (2003) 95; GARCÍA-MARTIN A. and SÁENZ J. J., *Phys. Rev. Lett.*, **87** (2001) 116603
- [4] MARKOŠ P., *Phys. Rev. Lett.*, **83** (1999) 588; RÜHLÄNDER M. *et al.*, *Phys. Rev. B*, **64** (2001) 212202
- [5] MARKOŠ P., *Phys. Rev. B*, **65** (2002) 104207; MARKOŠ P., *Anderson Transition and its Ramifications*, edited by T. BRANDES and S. KETTEMAN *Lecture Notes in Physics*, Vol. **630** (Springer) 2003
- [6] For a review, see LEE P. A. AND RAMAKRISHNAN T. V., *Rev. Mod. Phys.*, **57** (1985) 287
- [7] MUTTALIB K. A. *et al.*, *Ann. Phys. (NY)*, **308** (2003) 156
- [8] In Q1D systems, defined in [1–3, 12], disorder is always *weak* enough to assure that the localization length $\xi \gg L$ where L is the transverse dimension. The Q1D insulator corresponds to the *weakly disordered* systems of length $L_z \gg \xi$. This is different from localization in 3D which occurs at *strong* disorder, where $\xi \ll$ both L_z and L .
- [9] In ALTSHULER B. L. *et al.*, *Sov. Phys. JETP*, **64** (1986) 1352 and *Phys. Lett. A*, **134** (1989) 488, $P(g)$ has been considered in $d = 2 + \varepsilon$ dimensions where a completely log-normal distribution is expected at very large disorder. However, this result can not be extended to $d = 3$ [1, 16].
- [10] MUTTALIB K. A. and GOPAR V. A., *Phys. Rev. B*, **66** (2002) 115318; MUTTALIB K. A. and KLAUDER J. R., *Phys. Rev. Lett.*, **82** (1999) 4272
- [11] See e.g. STONE A. D. *et al.*, *Mesoscopic phenomena in solids*, edited by B. L. ALTSHULER, P. A. LEE and R. A. WEBB (North-Holland) 1991, p. 369
- [12] DOROKHOV O. N., *JETP Lett.*, **36** (1982) 318; MELLO P. A. *et al.*, *Ann. Phys. (N.Y.)*, **181** (1988) 290
- [13] The matrix k_{ab} depends on the representation α . Since localization is defined in configuration space, we choose the position representation.
- [14] PENDRY J. B. *et al.*, *Proc. R. Soc. London A*, **437** (1992) 67
- [15] PICHARD J.-L. *et al.*, *J. Phys. France*, **51** (1990) 587
- [16] MARKOŠ P. and KRAMER B., *Philos. Mag. B*, **68** (1993) 357
- [17] Note that for $|a - b| \gg L$, γ_{ab} must decrease as L^{-2} . From (2), $\sum_b K_{ab} = 1$ so the sum of L^2 *positive* parameters $\sum_b \gamma_{ab}$ is $\propto L^0$ in the insulating regime. We ignore this detail in our model.
- [18] CHALKER J. T. and BERNHARDT M., *Phys. Rev. Lett.*, **70** (1993) 982
- [19] We only consider orthogonal symmetry. As suggested in LERNER I. V. and IMRY Y., *Europhys. Lett.*, **29** (1995) 49 and KETTEMANN S. and RAIKH M. E., *Phys. Rev. Lett.*, **90** (2003) 146601, we expect non-trivial dependence of the localization length ξ on the universality class in 3D.
- [20] BEENAKKER C. W. J. and REJAEI B., *Phys. Rev. Lett.*, **71** (1993) 3689; *Phys. Rev. B*, **49** (1994) 7499
- [21] LANDAUER R., *IBM J. Res. Dev.*, **1** (1957) 223